In-situ photoconductivity measurement of imidazole in optical fiber break-junctions

Zhikai Zhao,[a] Chenyang Guo,[a] Lifa Ni,[a] Xueyan Zhao,[a] Surong Zhang[a] and Dong Xiang*[a]

[a.] *Tianjin Key Laboratory of Micro-scale Optical Information Science and Technology Institute of Modern Optics, Nankai University, Tianjin 300350, China.*

Electronic Supplementary Information

Table of contents

1. Fabrication processes of the F-MCBJ chips
2. The automatic measurement system
3. 2D histogram of molecular junctions
4. The optimization structures with various gap sizes
5. Evolution of MPSH states of imidazole monomer junction
6. Evolution of MPSH states of imidazole dimer junction
7. Conductance of the pi-pi stacking dimer junctions

1. Fabrication processes of the F-MCBJ chips

To fabricate the F-MCBJ chip, we first strip off the fiber cladding at one end of about 0.5 m optical fiber. We then place the optical fiber wiped with alcohol cotton in the optical fiber fusion splicer (FITEL S179), and taper the optical fiber to form an approximately 25 μm constriction, as shown in Fig. S1a. Subsequently, plasma cleaning and metal deposition processes are carried out. A layer of approximately 2 nm Cr and 50 nm Au is deposited on the top of the optical fiber by metal plasma sputtering, where the 2 nm Cr serves as the adhesion layer between optical fiber and the Au layer. The microscope photo of the constriction of metal-coated optical fiber is presented in Fig. S1b. A flexible substrate is prefabricated with three layers of PPA serving as the isolation layer, and a layer of PPA solution serving as a fixed layer. We press the fiber and heat it on a hot plate for 12 hours, the fiber will be fixed on the substrate. Top-view SEM image and side-view of metal-coated optical fiber is shown in Fig. S1c and Fig. S1d, respectively. There is a clear material boundary and a gap under the metallic bridge, if taking a close look at Fig. S1d.

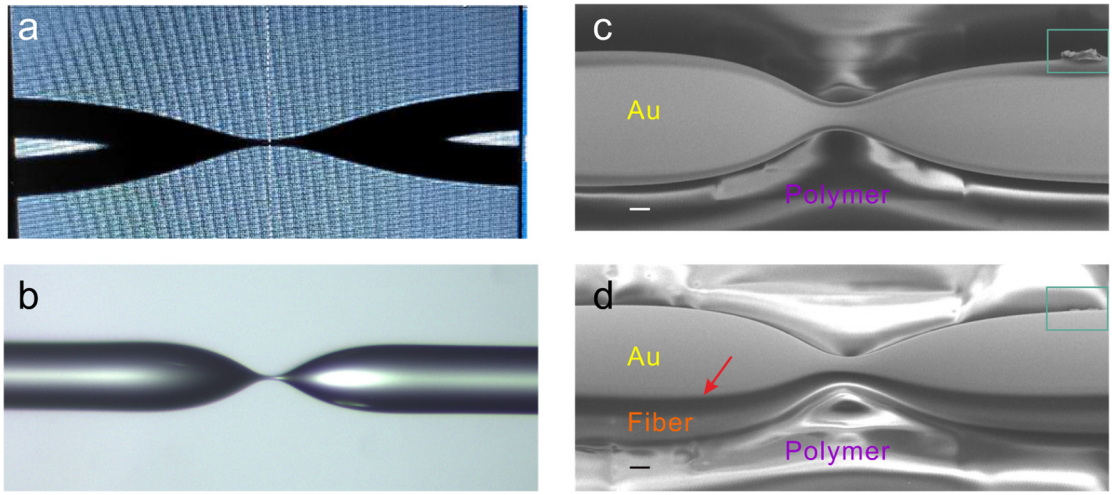

Fig. 1 (a) Schematic diagram of the tapering process. (b) Microscope photo of the constriction of metal-coated optical fiber. Top-view SEM image (c) and side-view (d) of metal-coated optical fiber. Scale bar: 20 μm. There is a clear material boundary and a gap under the metallic bridge in (d).

2. The automatic measurement system

We developed an automatic measurement system based on a current preamplifier, including three main modules. Here, we use a commercial precision DC voltage source (MODEL DC205) to apply a 18 mV bias voltage, and a 61 kΩ resistor is connected in series in the circuit as a protected resistor. The preamplifier (MODEL SR570) is set to 50 nA/V sensitivity, and a 24-bit data acquisition card (MC DT9824) is controlled by a PC to collect data with 4800 Hz sampling rate in real time. For the motion module, a piezo (N-111.2A) controlled by E-712 digital piezo controller is used.

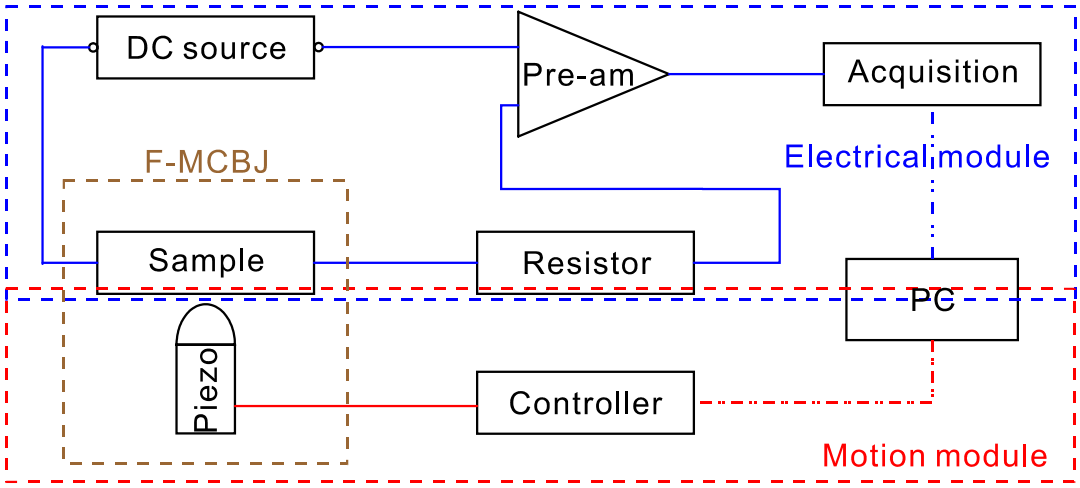

Fig. S2 Schematic diagram of measurement system.

3. 2D histogram of molecular junctions

2D histogram is able to include more useful information regarding the evolution of the molecular junction during stretching, thus, we plot 2D conductance histogram, as shown in Fig. S3. It can be found that the 2D histogram shows two main plateaus, corresponding to high molecular conductance (monomer junctions) and low molecular conductance (dimer junctions), respectively. A close examination of the 2D histogram, it can be further found that 1) the intensity of high conductance counts is higher than that of low conductance, as indicated by the red circles in Fig. S3. This observation indicates that the probability of forming monomer junctions is higher than that of dimer junctions; 2) the plateau length of low conductance is a little bit longer than that of high conductance. We attribute it to the fact that the length of dimer junctions is longer than the one of monomer junctions; and 3) the plateau of low conductance is right-shifted compared to the plateau of high conductance and partially overlaps each other on the time axis, which indicates that some dimer junctions are remained (or formed) after the break of monomer junction.

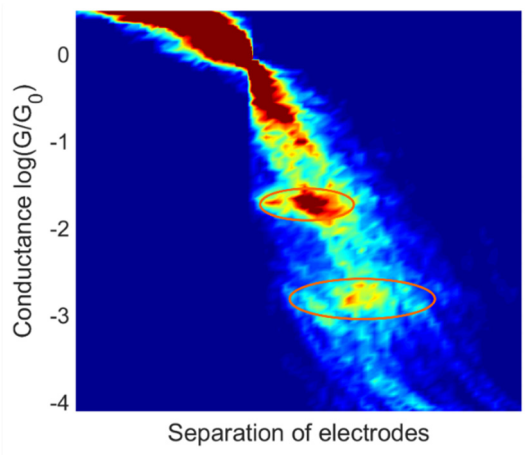

Fig. S3 2D conductance histogram of molecular junctions in the absence of light illumination. The circles indicate the two conductance plateaus. This 2D histogram is generated based on 500 curves (conductance as function of time).

4. The optimization structures with various gap sizes

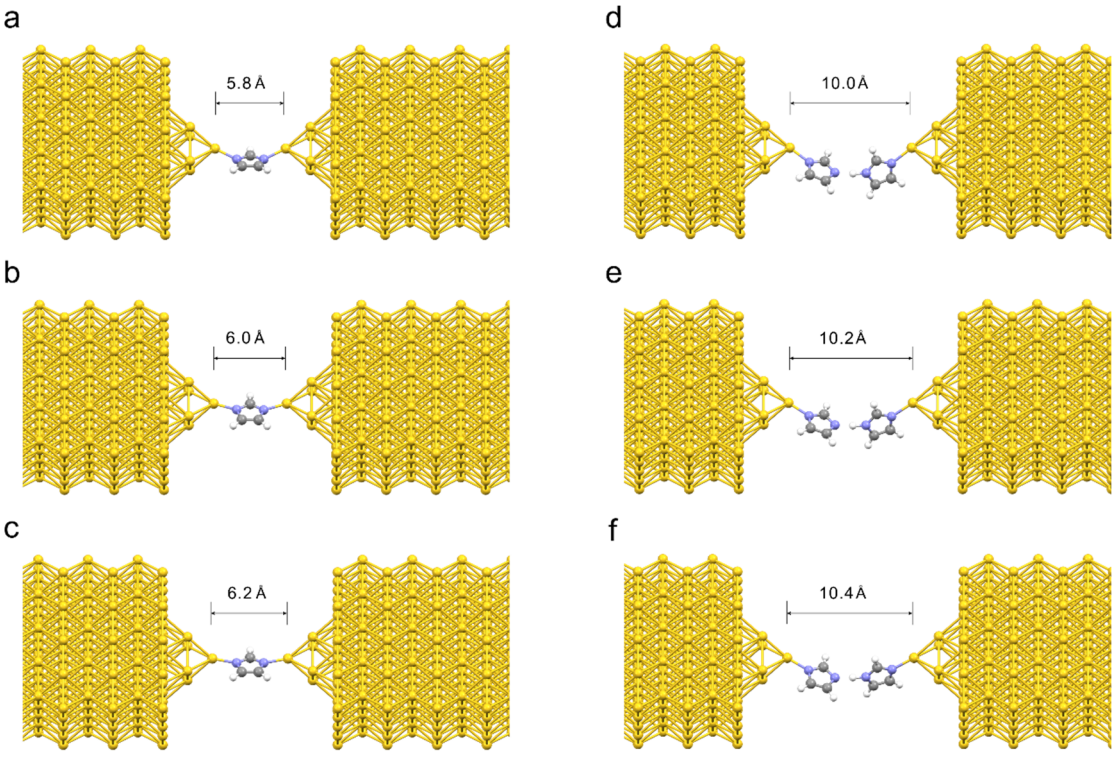

Fig. S4 Geometric optimization results for imidazole monomer junctions with 5.8 Å (a), 6.0 Å (b) and 6.2 Å (c). Geometric optimization results for imidazole dimer junctions with 10.0 Å (d), 10.2 Å (e) and 10.4 Å (f).

5. Evolution of MPSH states of imidazole monomer junction

The molecular projected self-consistent Hamiltonian (MPSH) and their energy eigenvalues were obtained from Transiesta codes. The energy eigenvalues of the frontier molecular orbitals remain relatively stable under various applied bias voltages, which result from the symmetrical structure of the imidazole monomer. The zero-bias MPSH states show obvious non-locality, which leads to the relatively high conductance for imidazole monomer junctions.

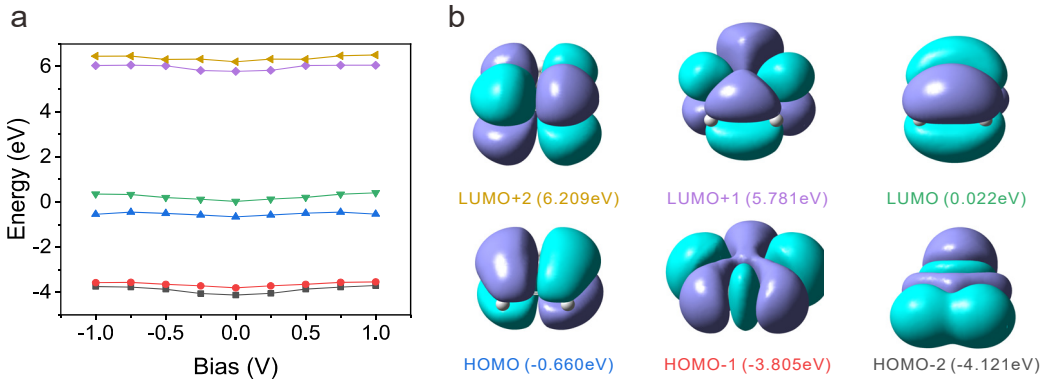

Fig. S5 (a) Evolution of the molecular projected self-consistent Hamiltonian (MPSH) states of imidazole monomer junction under various applied biases. The six lines from top to bottom show the energy of LUMO+2, LUMO+1, LUMO, HOMO, HOMO-1, HOMO-2, respectively. (b) zero-bias MPSH states and their energy eigenvalues of the imidazole monomer from HOMO-2 to LUMO+2 at 6.2 Å gap size. The isovalue for displaying wavefunctions of the frontier molecular orbitals is 0.02.

6. Evolution of MPSH states of imidazole dimer junction

Comparing with MPSH states of imidazole monomer junction presented in Fig. S5b, the MPSH states of imidazole dimer junction is localized, which can explain the poor conductance of imidazole dimer junctions. Moreover, the evolution of the MPSH states is bias-dependent. Specifically, the energy will change synchronously with the chemical potential of the electrode, on which the wavefunction is more localized.

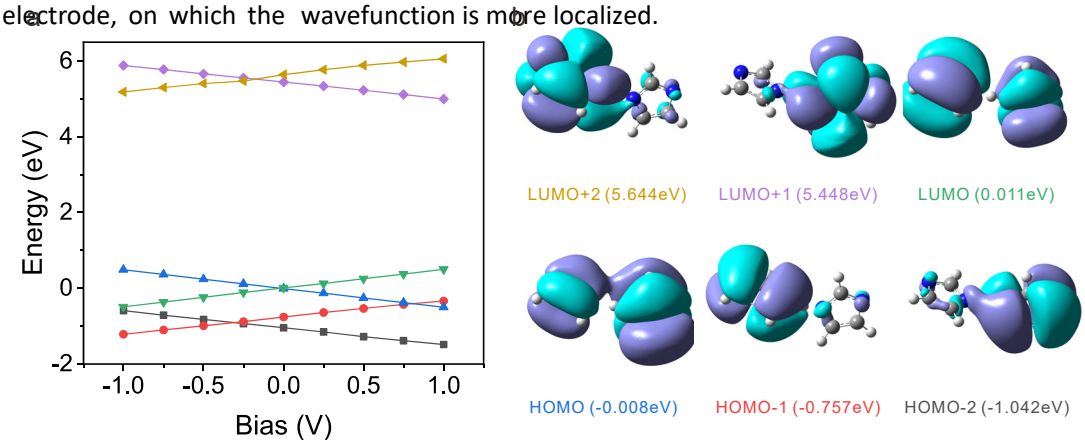

Fig. S6 (a) Evolution of the molecular projected self-consistent Hamiltonian (MPSH) states of imidazole dimer junction under various applied biases. (b) zero-bias MPSH states and their energy eigenvalues of the imidazole dimer from HOMO-2 to LUMO+2 at 10.2 Å gap size. The isovalue for displaying wavefunctions of the frontier molecular orbitals is 0.02.

7. Conductance of the pi-pi stacking dimer junctions

As a planar 5-membered ring, imidazole can form the pi-pi stacking dimer. Thus, we do the optimizations and transport calculations of a pi-pi stacking dimer with different gap sizes (7.1 Å and 7.5 Å). Theoretical simulations reveal that the conductance of pi-pi stacking molecular junctions does not match the "L" peak in histograms, since the calculated conductance is much lower than the peak value presented in the histogram and is may beyond the current detective window. The weak coupling of pi-pi stacking leads to a relatively low probability of forming molecular junctions and a low conductance overwhelmed by background noise.

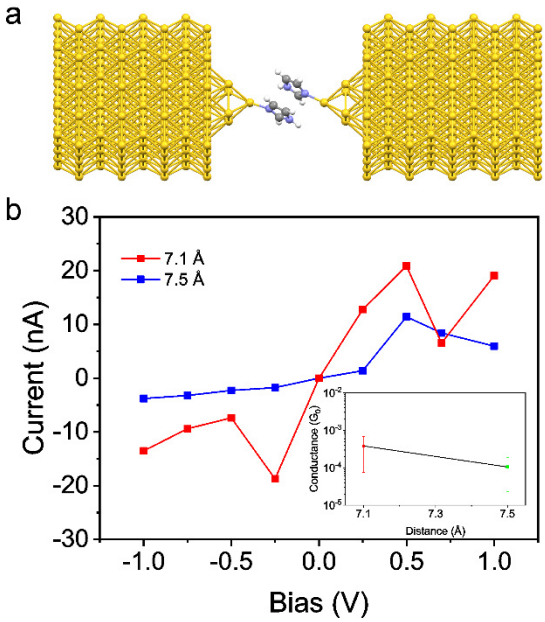

Fig. S7 (a) Geometric optimization result of pi-pi stacking imidazole molecular junction. (b) Calculated current-voltage characteristics and conductance for pi-pi stacking imidazole dimer junctions under different gap sizes.